Materials Science-Poland, 33(1), 2015, pp. 198-204
http://www.materialsscience.pwr.wroc.pl/
DOI: 10.1515/msp-2015-0013

DE GRUYTER OPEN

Influence of aluminium concentration in $Zn_{0.9}V_{0.1}O$ nanoparticles on structural and optical properties

A. SAYARI[1,2*], L. EL MIR[3,4], S. AL-HENITI[5], T. AL-HARBI[5], S. J. YAGHMOUR[1], A.A. AL-GHAMDI[5]

[1]Department of Physics, Faculty of Science, King Abdulaziz University , North Jeddah Branch, P.O. Box 80203, Jeddah 21589, Kingdom of Saudi Arabia

[2]Equipe de Spectroscopie Raman, Département de Physique, Faculté des Sciences de Tunis, Campus Universitaire, El-Manar, 2092 Tunis, Tunisie

[3]Al Imam Mohammad Ibn Saud Islamic University (IMSIU), College of Sciences, Department of Physics, Riyadh 11623, Saudi Arabia

[4]Laboratoire de Physique des Matériaux et des Nanomatériaux appliquée à l'Environnement, Faculté des Sciences de Gabès, Cité Erriadh Manara Zrig, 6072 Gabès, Tunisia

[5]Department of Physics, Faculty of Science, King Abdulaziz University, P.O. Box 80203, Jeddah 21589, Kingdom of Saudi Arabia

The (V,Al) co-doped ZnO nano-structured powders ($Zn_{0.9-x}V_{0.1}Al_xO$, where x = 0.02, 0.03 and 0.04) were synthesized via the sol-gel technique and their structural and optical properties were investigated. The effect of Al concentration on the structural and optical properties of the $Zn_{0.9-x}V_{0.1}Al_xO$ nanopowders was studied using various techniques. The XRD patterns indicate that the samples have a polycrystalline wurtzite structure. The crystallite size increases with increasing the Al content and lies in the range of 23 to 30 nm. The lattice strain, estimated by the Stokes-Wilson equation, decreases when Al content increases. SEM and TEM micrographs show that $Zn_{0.9-x}V_{0.1}Al_xO$ powders are the agglomeration of nanoparticles having spherical and hexagonal shapes with dimensions ranging from 20 to 30 nm. FT-IR spectra show a distinct absorption peak at about 500 cm^{-1} for ZnO stretching modes and other peaks related to OH and H_2O bands. Raman spectra confirm the wurtzite structure of the $Zn_{0.9-x}V_{0.1}Al_xO$ nanoparticles. The direct band gaps of the synthesized $Zn_{0.9-x}V_{0.1}Al_xO$ nanopowders, estimated from the Brus equation and the crystallite sizes deduced from XRD, are around 3.308 eV. The decomposition process of the dried gel system was investigated by thermal gravimetric analysis (TGA).

Keywords: *ZnO nanopowder; V and Al co-doping; XRD; TEM; Raman scattering*

1. Introduction

In recent years, nanostructure materials have attracted a great deal of attention because of their versatile and remarkable physical, optical and electronic properties. Particularly, ZnO is a wide band gap semiconductor (3.3 eV) with a high exciton binding energy (60 meV) at room temperature, which has received more and more attention in the material science due to its various expected applications. ZnO nanomatererials have been realized by various techniques including thermal evaporation [1], chemical vapor deposition [2], sputtering [3], spray pyrolysis [4], pulsed laser deposition [5] and sol gel processes [6–8]. Among these methods, the sol gel process is particularly attractive because of its simplicity and acceptable costs for the large scale fabrication of nanostructure ZnO.

Doping is an effective method to modify the physical properties of a base material in order to extend its applications. Relevant reports on ZnO doped with group IIIA, VB, VIIB and VIIIB metals, such as Al, V, Mn and Co indicate that the doping effect improves the optical, electrical and magnetic properties of the ZnO [9–11].

*E-mail: amor.sayari@laposte.net

Additionally, Al doped ZnO films are useful materials for variety of applications, including transparent electrodes in flat panel displays, light emitting diodes, solar cells and gas sensors [12–15]. Al doped nanomaterials, which are nontoxic, high transparent and low cost materials, have competitive properties as compared to indium tin oxide. Thus, investigations on optical, structural and vibrational properties of Al doped ZnO nanostructure materials are of great importance. However, the investigation of doping and co-doping effects on the morphology and other properties is actually insufficient and needs further studies. Few works on ZnO films co-doped with Al and transition metals have been devoted to the study on their optical, electrical and magnetic properties [16, 17]. The Al and transition metal co-doped ZnO films are important functional materials for optoelectronic and magnetoelectronic applications. The usually used transition metals are Co, Mn and V.

In this research, we have investigated (V,Al) co-doped ZnO nanopowders ($Zn_{0.9-x}V_{0.1}Al_xO$, where x = 0.02, 0.03 and 0.04) synthesized by the sol-gel process in order to study the change in the shape, structure and optical properties of resulting materials. The morphology and structure of the Zn(V,Al)O nanopowders were studied using scanning electron microscopy (SEM) and X-ray diffraction (XRD). The optical and thermal analysis measurements of the nanopowder samples were measured using an FT-IR spectrophotometer and a thermal gravimetric analyzer. All the results have been discussed in relation to doping concentrations.

2. Experimental details

(V,Al) co-doped ZnO nanocrystals were prepared by the sol-gel method using 16 g of zinc acetate dehydrate as a precursor in 112 mL of methanol. After 10 min magnetic stirring at room temperature, 0.628 g of ammonium metavanadate corresponding to [V]/[Zn] = 0.10 and adequate quantities of aluminium nitrate-9-hydrate corresponding to [Al]/[Zn] ratios of 0.02, 0.03 and 0.04 were added. After an additional 15 min magnetic stirring, the solution was placed in an autoclave and dried under supercritical conditions of ethyl alcohol (EtOH). The obtained powder was then heated in a furnace at 500 °C for 2 hours in air.

Crystallite phase and orientation were evaluated by X-ray diffraction (Philips X'pert diffractometer) supplied with copper X-ray tube ($\lambda_{k\alpha 1}$ = 1.5406 Å), nickel filter, graphite crystal monochromator, proportional counter detector, divergence slit 1° and 0.1 mm receiving slit. The working conditions were 40 kV and 30 mA for the X ray tube, scan speed 0.05° and 2 s measuring time per step. The transmission electron microscopy (TEM) measurements were performed with a JEM-200CX microscope. The Raman spectra were performed at room temperature with a Labram system equipped with a microscope in backscattering configuration. The excitation line at 514.5 nm was from an Ar^+ laser. FT-IR spectroscopy (Thermo Scientific Nicolet iS10 FT-IR Spectrometer) was used at room temperature in the range of 450 to 4000 cm^{-1} with a resolution of 4 cm^{-1}. Thermal gravimetric analysis (TGA) curves of the (V,Al) co-doped ZnO nanopowders were obtained using a TG-DTA apparatus (PerkinElmer). Approximately 2.9 mg of a sample was placed in a platinum crucible on the pan of a microbalance and heated from 35 to 950 °C at a rate of 10 °C·min^{-1}.

3. Results and discussions

3.1. Structural and morphological characterization

Typical XRD patterns obtained for various samples of $Zn_{0.9-x}V_{0.1}Al_xO$ nanocrystals are shown in Fig. 1. Except the intensity reduction and a slight shift of XRD peaks to higher angles for the sample $Zn_{0.9-x}V_{0.1}Al_xO$ (x = 0.03), no difference in XRD patterns was found in the other samples (x = 0.02 and 0.04). For each sample, the reflection peaks show completely hexagonal wurtzite structure with no secondary phases (related to V and/or Al atoms) within the detection limit of our XRD [18]. The XRD measurements indicate that these nano-sized $Zn_{0.9-x}V_{0.1}Al_xO$ particles are highly crystallized and all the

diffraction peaks match well with Bragg reflections of the standard wurtzite-type ZnO structure [18]. The crystallite size of the $Zn_{0.9-x}V_{0.1}Al_xO$ nanopowders (d), calculated from the widths of the major diffraction peaks observed in Fig. 1 using the Scherrer formula [19], are given in Table 1. The average crystallite sizes range from 23 to 30 nm. From Table 1 it is clear that crystallite size increases with increasing the Al content.

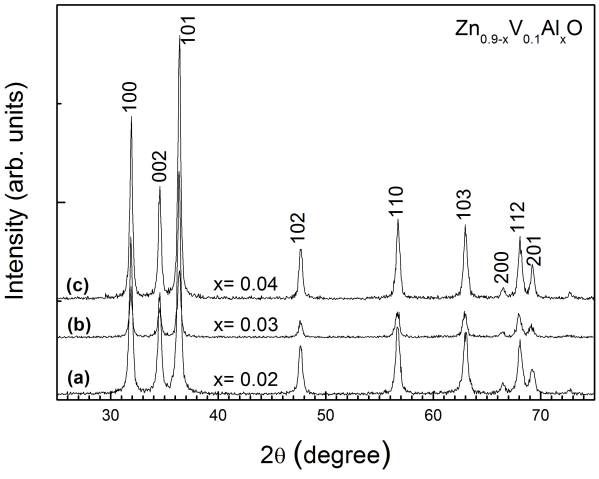

Fig. 1. The XRD patterns of the three $Zn_{0.9-x}V_{0.1}Al_xO$ nanopowders synthesized by the sol-gel process. (a) x = 0.02, (b) x = 0.03 and (c) x = 0.04.

For all the $Zn_{0.9-x}V_{0.1}Al_xO$ nanoparticles the lattice parameters, given in Table 2, are slightly smaller than those of pure ZnO. Certainly, the incorporation of V and Al ions, which have smaller sizes than that of Zn, is responsible for the observed effect. Moreover, it is seen from Table 2 that the lattice constants slightly decrease at x = 0.03 compared to those for x = 0.02 and 0.04. The ratio of a/c of $Zn_{0.87}V_{0.1}Al_{0.03}O$ is 0.623, which is slightly smaller than that of pure ZnO (0.624), which might be due to the incorporation of more Al ions for this Al composition (x = 0.03). This is confirmed by the small shift in XRD peaks for x = 0.03 (Fig. 1), which implies systematic replacement of Zn ions by Al ions in the lattice without changing its wurtzite structure. The lattice strain was also calculated according to Stokes-Wilson equation and is given in Table 1. We note that this parameter decreases when the Al content increases in accordance with the increase of the grain size. Fig. 2 shows SEM images of the $Zn_{0.9-x}V_{0.1}Al_xO$ nanopowders. The nanoparticle morphology does not change significantly with increasing Al content. SEM images show a mixture of nanoparticles, where the grains have different sizes and shapes (spherical and hexagonal). The largest portion of the powder is agglomerated, but some separated particles are also found (Fig. 2). According to the SEM analysis, hexagonal prismatic particles with a broad particle size distribution are observed (Fig. 2b). The aerogel powders are composed of nanometer sized particles as confirmed by TEM micrograph of the $Zn_{0.87}V_{0.1}Al_{0.03}O$ sample (Fig. 3a). The grain size estimated using TEM micrographs and the 100 nm scale bar ranges from 20 to 30 nm. The later values are very similar to those deduced from XRD measurements and the Scherrer equation (Table 1). The EDX spectrum of the $Zn_{0.87}V_{0.1}Al_{0.03}O$ sample, presented as example in Fig. 3b, shows signals directly related to the dopants. Zn and O appear as the main components with low levels of V and Al, which confirms the formation of Al and V co-doped ZnO.

In order to extract the band gap energy (E_g) of the $Zn_{0.9-x}V_{0.1}Al_xO$ nanopowder samples, the values of the crystallite sizes obtained from XRD measurements have been inserted into the Brus equation, which is derived from the effective mass model [20]. The obtained values of E_g, listed in Table 2, are around 3.308 eV. The different parameters of ZnO bulk used in the Brus equation were taken from [21].

3.2. TGA analysis

The thermal behavior of dried Zn(V,Al)O gel has been investigated by thermal gravimetric analysis (TGA). Fig. 4 depicts the results of the TGA measurements of the nano-sized $Zn_{0.9-x}V_{0.1}Al_xO$ particles. It can be seen that the sample weight decreases continuously with the increase in temperature before reaching a stable value at 700 °C (Fig. 4). The TGA curves of all the samples show two weight loss stages between 100 and 410 °C, and between 410 and 700 °C. The mass losses for the temperature range of 100 to 410 °C are ∼3, 5

Table 1. The crystallite sizes and the lattice strain estimated from XRD data along the major reflection planes of the three $Zn_{0.9-x}V_{0.1}Al_xO$ samples.

Nominal Al concentration (at.%)	(101)		(100)		(002)	
	Crystallite size d(nm)	Lattice strain ($\times 10^{-3}$)	Crystallite size d(nm)	Lattice strain ($\times 10^{-3}$)	Crystallite size d(nm)	Lattice strain ($\times 10^{-3}$)
2	23.35	4.71	24.42	5.11	22.91	5.04
3	24.08	4.49	26.59	4.76	23.02	4.94
4	28.76	3.82	29.90	4.17	28.84	4.01

Table 2. Lattice parameter values calculated from the XRD patterns and the energy gap of (V, Al) co-doped ZnO nanopowders. The energy gap was estimated from the effective mass model (Brus equation) and the crystallite size of the nanopowder sample.

Nominal Al concentration (at.%)	Energy gap (eV)	Lattice parameters (Å)	
		a	c
2	3.307	3.2385	5.1874
3	3.308	3.1862	5.1112
4	3.313	3.2356	5.1853

and 6 % for x = 0.02, 0.03 and 0.04, respectively. While in the temperature range of 410 to 700 °C, the mass losses are ∼7, 8 and 9 % for x = 0.02, 0.03 and 0.04, respectively. The first weight loss stage corresponds to the dehydration of $Zn_{0.9-x}V_{0.1}Al_xO$ nanopowders and decomposition of zinc acetate by combustion. However, the second stage is related to the release of entrapped gases formed during the decomposition of acetate ions [22]. The obtained residue is around 90 % (pure ZnO phase).

3.3. Raman scattering

Room temperature Raman spectra of Zn(V,Al)O nanopowders, synthesized by the sol-gel process, are shown in Fig. 5. At the low frequency region, the peaks at 180, 320, 370, 410 and 433 cm^{-1} are attributed, respectively, to the $2E_2$(low), $2E_2$(M), A_1(TO), E_1(TO) and E_2(high) modes [23]. The observation of the later modes indicates that the Zn(V,Al)O product has a wurtzite structure as confirmed by XRD analysis [24]. The intense peak around 713 cm^{-1} can be assigned to combinations of LA and TO modes at the M point. The relatively intense peak located at about 500 cm^{-1} could be assigned to multiphonon scattering of the E_1 (TO) and E_2 (low) modes. Phonons in a nanocrystal are confined in space and all types of phonons over the entire Brillouin zone contribute to the Raman spectrum. The Raman peak at 576 cm^{-1} may be due to the A_1(LO) mode [25]. Recent reports have considered the appearance of this mode in relation to lattice defects, being either oxygen vacancies or zinc interstitials or their combination [26, 27].

3.4. FT-IR measurements

Fig. 6 illustrates the FT-IR spectra of the $Zn_{0.9-x}V_{0.1}Al_xO$ nanopowder samples in the range of 500 to 4000 cm^{-1} at room temperature. In the FT-IR spectra of the synthesized products, there is a significant spectroscopic band at around 500 cm^{-1}. This is the characteristic band of ZnO [28]. The peak at 680 cm^{-1} is probably due to nitrate (NO_3^-) group, which has not completely been removed during the sol-gel process. Also, the characteristic absorption bands at about 3400, 1560 cm^{-1}, corresponding to the O–H stretching and bending modes of water absorbed on the surface of nanocrystals, respectively, are observed [29]. The weak absorption at 1409 cm^{-1} is attributed to the C=O stretching mode [30]. However, the band arising from the absorption of atmospheric CO_2 on the metallic cations is clearly observed at 2303 cm^{-1}.

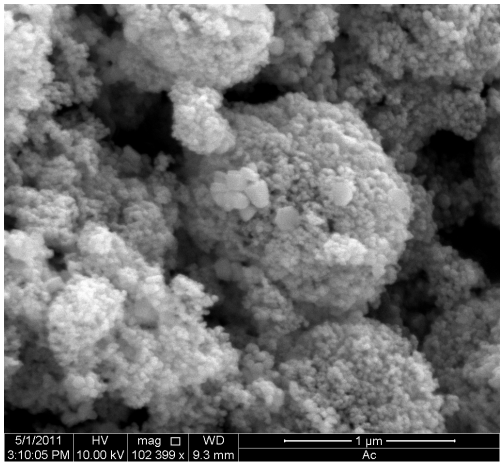

(a)

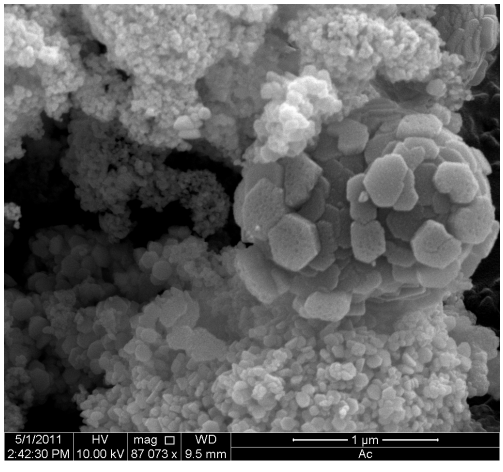

(b)

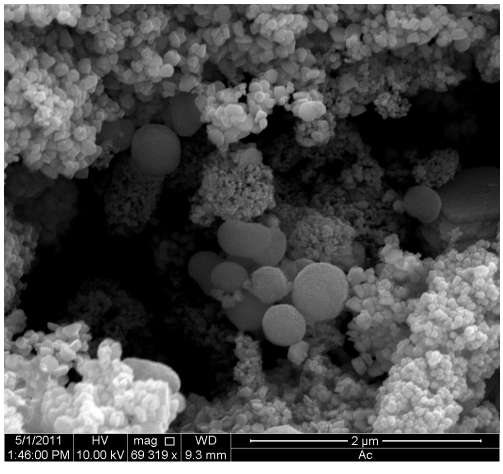

(c)

Fig. 2. Typical SEM micrographs showing the morphology of nanocrystalline $Zn_{0.9-x}V_{0.1}Al_xO$ samples (a) x = 0.02, (b) x = 0.03, and (c) x = 0.04.

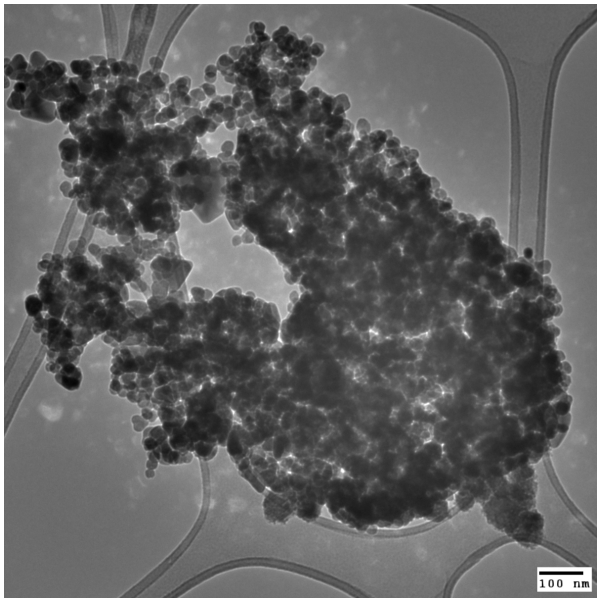

(a)

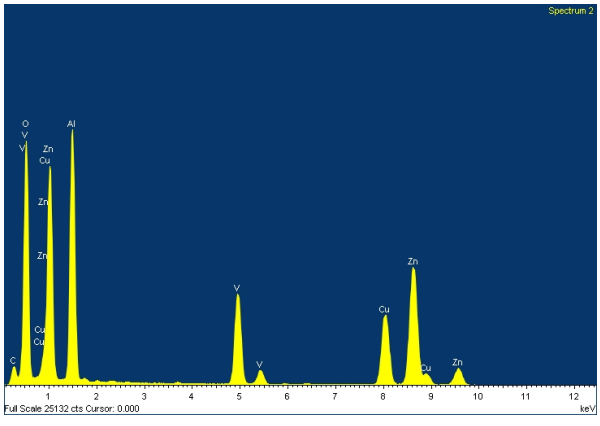

(b)

Fig. 3. TEM micrograph (a) and EDX analysis (b) of the synthesized $Zn_{0.9-x}V_{0.1}Al_xO$ nanoparticles for x= 0.03.

4. Conclusion

In summary, $Zn_{0.9-x}V_{0.1}Al_xO$ nanopowders with crystallite size in the range of 23 to 30 nm were prepared at various Al concentrations (2, 3 and 4 at.%) using the sol-gel technique. The protocol of elaboration was based on slow hydrolysis of the precursor using an esterification reaction, followed by a supercritical drying in EtOH. The properties of the powder samples were discussed in details. The effect of various aluminum concentrations on the structure, morphology and

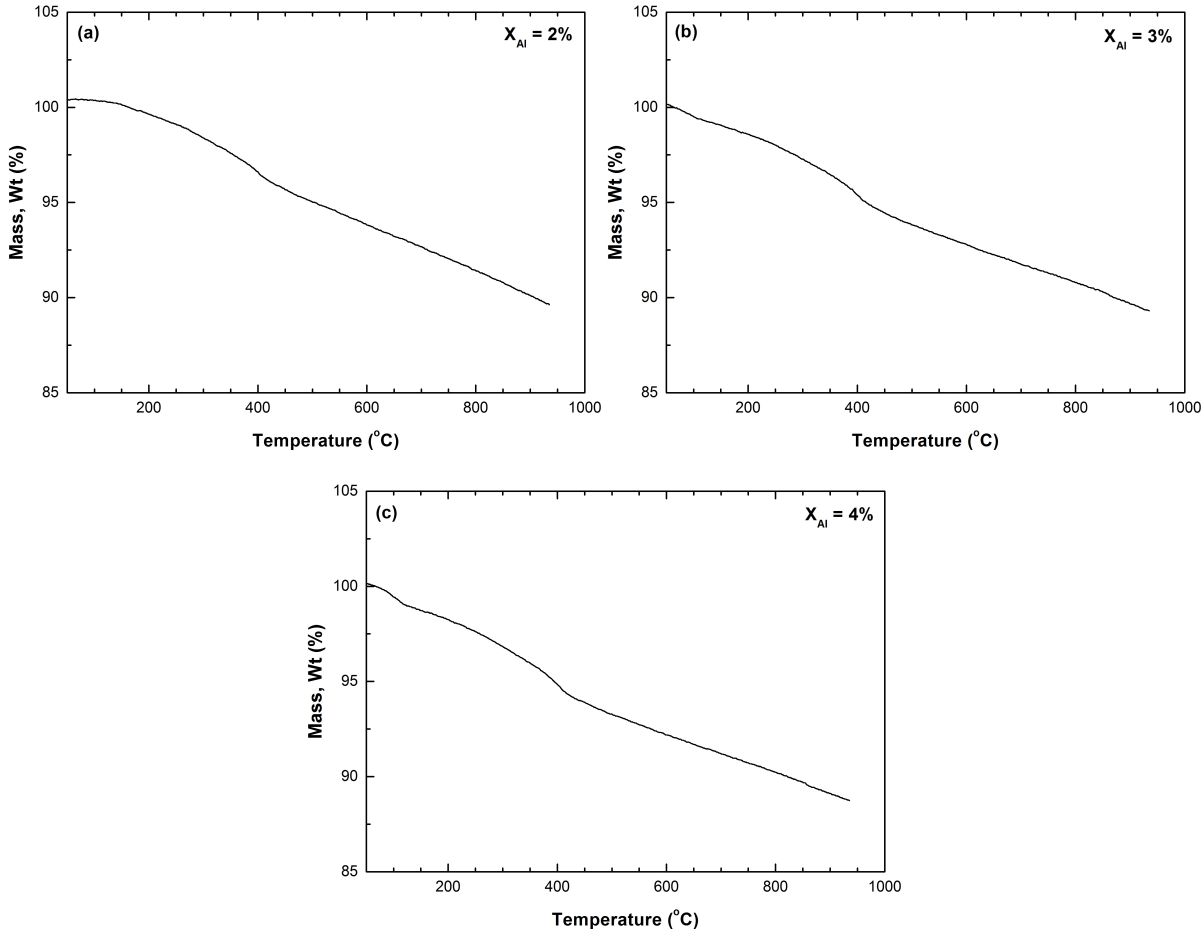

Fig. 4. TGA curves of nano-sized $Zn_{0.9-x}V_{0.1}Al_xO$ powders at a heating rate of 10 °C/min. (a) x = 0.02, (b) x = 0.03 and (c) x = 0.04.

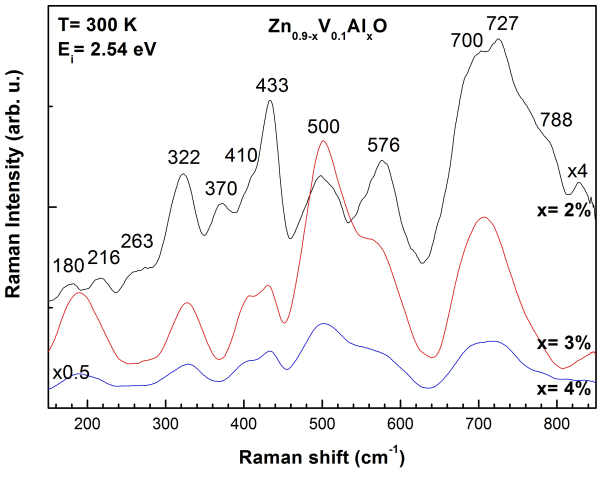

Fig. 5. Room temperature Raman backscattering spectra of the nanocrystalline $Zn_{0.9-x}V_{0.1}Al_xO$ powders.

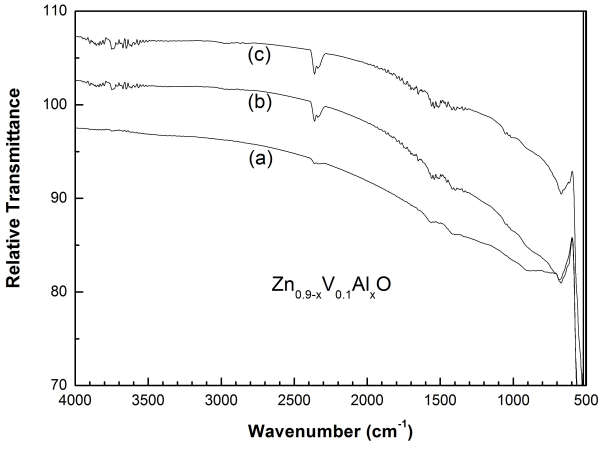

Fig. 6. FT-IR spectra of $Zn_{0.9-x}V_{0.1}Al_xO$ nanoparticles. The spectra were recorded at room temperature and vertically shifted for clarity. (a) x = 0.02, (b) x = 0.03, and (c) x = 0.04.

optical properties of the samples was studied. The XRD patterns of $Zn_{0.9-x}V_{0.1}Al_xO$ nanopowders revealed that the products had a single-crystalline wurtzite hexagonal structure. The XRD measurements showed that at x = 0.3, higher amount of Al ions were incorporated into the ZnO lattice. The SEM and TEM images showed the surface topography of the elaborated $Zn_{0.9-x}V_{0.1}Al_xO$ nanopowders, which were formed of nanoparticles having spherical and hexagonal shapes and assembled in agglomeration. The nanocrystalline $Zn_{0.9-x}V_{0.1}Al_xO$ powders obtained in this study, exhibited direct optical band gap around 3.308 eV. Thermal analysis showed that the obtained residue contained around 90 % of pure ZnO phase. Raman and FT-IR measurements confirmed the formation of the wurtzite phase $Zn_{0.9-x}V_{0.1}Al_xO$ nanoparticles.

References

[1] TONOOKA K., BANDO H., AIURA Y., *Thin Solid Films*, 445 (2003), 327.

[2] PARK J.H., JANG S.J., KIM S.S., LEE B.T., *Appl. Phys. Lett.*, 89 (2006), 121108.

[3] YU Z.G., WU P., GONG H., *Appl. Phys. Lett.*, 88 (2006), 132114.

[4] JOSPH B., GOPCHANDRAN K.G., THOMAS P.V., KOSHY P., VAIDYAN V.K., *Mater. Chem. Phys.*, 58 (1999), 71.

[5] CHEN J.J., YU M.H., ZHOU W.L., SUN K., WANG L.M., *Appl. Phys. Lett.*, 87 (2005), 173119.

[6] EL MIR L., GHRIBI F., HAJIRI M., BEN AYADI Z., DJESSAS K., CUBUKCU M., VON BARDELEBEN H.J., *Thin Solid Films*, 519 (2011), 5787.

[7] SAYARI A., EL MIR L., *KONA Powder Part. J.*, 32 (2015), DOI:10.14356/kona.2015003.

[8] EL MIR L., BEN AYADI Z., RAHMOUNI H., EL GHOUL J., DJESSAS K., VON BARDELEBEN H.J., *Thin Solid Films*, 517 (2009), 6007.

[9] SRINIVASAN G., RAJENDRA KUMAR R.T., KUMAR J., *Opt. Mater.*, 30 (2007), 314.

[10] ARREDONDO E.J.L., MALDONADO A., ASOMOZA R., ACOSTA D.R., LIRA M.A.M., OLVERA L., *Thin Solid Films*, 490 (2005), 132.

[11] YUAN G.D., ZHANG W.J., JIE J.S., FAN X., TANG J.X., LEE C.S., LEE S.T., *Adv. Mater.*, 20 (2008), 168.

[12] MINAMI T., *Thin Solid Films*, 516 (2008), 5822.

[13] CHUA B.S., XU S., REN Y.P., CHENG Q.J., OSTRIKOV K., *J. Alloy. Compd.*, 485 (2009), 379.

[14] CHEN M., PEI Z.L., SUN C., GONG J., HUANG R.F., WEN L.S., *Mater. Sci. Eng. B-Adv.*, 85 (2001), 212.

[15] SONG D., ABERLE A.G., XIA J., *Appl. Surf. Sci.*, 195 (2002), 291.

[16] EL GHOUL J., BOUGUILA N., GÓMEZ-LOPERA S.A., EL MIR L., *Superlattice. Microst.*, 64 (2013), 451.

[17] WOO L.J., HUI K.N., HUI K.S., CHO Y.R., HWAN C.H., *Appl. Surf. Sci.*, 293 (2014), 55.

[18] SHEN G.Z., CHO J.H., YOO J.K., YI G.C., LEE C.J., *J. Phys. Chem. B*, 109 (2005), 5491.

[19] CULLITY B.D., STOCK S.R., *Elements of X-ray Diffraction*, Prentice Hall, New York, 2001.

[20] BRUS L.E., *J. Chem. Phys.*, 80 (1984), 4403.

[21] STUDENIKIN S.A., GOLEGO N., COCIVERA M., *J. Appl. Phys.*, 84 (1998), 2287.

[22] BARICK K., ASLAM M., DRAVID V., BAHADUR D., *J. Phys. Chem. C*, 112 (2008), 15163.

[23] CALLEJA J.M., CARDONA M., *Phys. Rev. B*, 16 (1977), 3753.

[24] DAMEN T.C., PORTO S.P.S., TELL B., *Phys. Rev.*, 142 (1966), 570.

[25] CUSCO R., ALARCON-LLADO E., IBANEZ J., ARTUS L., JIMENEZ J., WANG B., CALLAHAN M.J., *Phys. Rev. B*, 75 (2007), 165202.

[26] CHEN Z.Q., KAWASUSO A., XU Y., NARAMOTO H., YUAN X.L., SEKIGUCHI T., SUZUKI R., OHDAIRA T., *Phys. Rev. B*, 71 (2005), 115213.

[27] KASCHNER A., HABOECK U., STRASSBURG M., KACZMARCZYK G., HOFFMANN A., THOMSEN C., ZEUNER A., ALVES H.R., HOFMANN D.M., MEYER B.K., *Appl. Phys. Lett.*, 80 (2002), 1909.

[28] GUPTA T.K., *J. Mater. Res.*, 7 (1992), 3280.

[29] GOSWAMI N., SEN P., *Solid State Commun.*, 132 (2004), 791.

[30] BALACHANDRA KUMAR K., RAJI P., *Recent Res. Sci. Technol.*, 3 (2011), 48.

Received 2014-02-08
Accepted 2014-10-19